

~~RESTRICTED~~

RM No. L8I17

UNCLASSIFIED

NOV 24 1948

NACA**RESEARCH MEMORANDUM**

A METHOD FOR CALCULATING FLOW FIELDS OF COWLINGS

WITH KNOWN SURFACE-PRESSURE DISTRIBUTIONS

By

Robert W. Boswinkle, Jr.

Langley Aeronautical Laboratory
Langley Field, Va.

CLASSIFICATION CANCELLED

Authority

J. W. Crowley
*EO 145011*Date *12/1/48* 3

By

J. H. 1/12/54
RF-2008

Sec

This document contains classified information affecting the National Defense of the United States within the meaning of the Espionage Act, USC 501 and 502. Its transmission or the revelation of its contents in any manner to an unauthorized person is prohibited by law. Information so classified may be imparted only to persons in the military and naval services of the United States, appropriate civilian officers and employees of the Federal Government who have a legitimate interest therein, and to United States citizens of known loyalty and discretion who of necessity must be informed thereof.

**NATIONAL ADVISORY COMMITTEE
FOR AERONAUTICS**

WASHINGTON

November 22, 1948

LANGLEY AERONAUTICAL LABORATORY

Langley Field, Va.

~~RESTRICTED~~

UNCLASSIFIED



NATIONAL ADVISORY COMMITTEE FOR AERONAUTICS

RESEARCH MEMORANDUM

A METHOD FOR CALCULATING FLOW FIELDS OF COWLINGS
WITH KNOWN SURFACE-PRESSURE DISTRIBUTIONS

By Robert W. Boswinkle, Jr.

SUMMARY

The present paper describes a way in which the data of three previous reports may be utilized to compute the incompressible flow fields for cowl-spinner combinations and open-nose inlets for use in the design of propeller shanks and cuffs. The paper also shows in general how the flow field of an unyawed body of revolution may be found if its pressure distribution is known, and presents the field of a ring vortex, which is used in these calculations, in a more convenient form than in the paper from which it was obtained.

The method consists of regarding the cowl surface as replaced by a ring vortex sheet whose strength at any point is equal to the local tangential velocity. The field of the ring vortex sheet is integrated to give the induced velocities of the body.

The accuracy of the method is verified by a comparison with experimental results. The method is rigorous only for axially symmetric bodies at zero angle of attack, but an approximate method yields results that agree with experimental values at radii greater than the maximum cowl radius at 10° angle of attack.

The application of the Prandtl-Glauert rule for calculating the compressible flow field in regions where the deviations of the pressures from the free-stream conditions are small is given in detail.

INTRODUCTION

In the design of propellers having airfoil-type shanks, an accurate knowledge of the velocities and directions of the air flow in the region of the spinners is necessary if the possible gains from such designs are actually to be realized. Part of the induced flow is contributed by the propeller itself; this part will not be treated in the present study. The remainder, which in any case is the main part for the very important

~~RESTRICTED~~

UNCLASSIFIED

high-speed-flight condition is contributed by the body; it accordingly becomes important to be able to calculate the flow about a cowl configuration in the neighborhood of the spinner.

A number of studies exist which describe satisfactory methods for computing the flow about simple closed bodies of revolution at zero incidence (references 1 to 5). Corresponding calculations for an open-nose body (which are desirable for a rotating cowl, the type of cowl in which the forward part rotates with the propeller) are much more difficult, and the procedure suggested in reference 6, in which a distribution of source and vortex rings must first be sought that will adequately represent the cowl, seems very unattractive with regard to computational tedium. For the more important and very much more difficult case of the cowl-spinner combinations, in which two separate bodies, the cowl and the spinner, contribute to the field, no solution has yet been offered. The flow about open-nose inlets and cowl-spinner combinations at zero incidence, however, may be calculated without excessive effort if, in addition to the specified body shapes, the velocities along the body surfaces are also given.

Surface velocities may be obtained for a range of cowl-spinner combinations and open-nose inlets at a large number of inlet-velocity ratios from two recent publications (references 7 and 8). The present paper describes a way in which these data and the data of reference 9, which gives in detail the flow field of a ring vortex, can be used to compute the desired cowl flow fields. In addition, the paper shows generally how the flow field about an unyawed body of revolution can be found if its pressure distribution is known and presents the data of reference 9 in a somewhat more convenient form.

SYMBOLS

D	maximum cowl diameter
M	Mach number in undisturbed stream
p	static pressure
p_o	static pressure in undisturbed stream
P	static pressure coefficient $\left(\frac{p - p_o}{q_o} \right)$
q_o	dynamic pressure in undisturbed stream
r	radial ordinate of point in field, measured from axis of symmetry

r'	radius of ring vortex
s	distance along cowling meridian
s'	distance along spinner meridian
u	axial induced velocity component
u^*	axial induced velocity component for a ring vortex of radius r' and strength $2\pi r'$
v	radial induced velocity component
v^*	radial induced velocity component for a ring vortex of radius r' and strength $2\pi r'$
x	axial distance from ring vortex to point in field
V_1/V_0	inlet-velocity ratio, ratio of average velocity of flow in inlet to velocity in undisturbed stream
V_2/V_0	flow-speed ratio, ratio of local flow speed at point in field to velocity in undisturbed stream
V_s/V_0	surface velocity ratio, ratio of velocity of flow just outside the boundary layer at point on cowling or spinner surface to velocity in undisturbed stream
α	angle of attack of axis of symmetry, degrees
γ	strength of ring vortex
ϕ	flow divergence angle, referred to axis of symmetry (positive outward), degrees

THEORY

The irrotational motion of an incompressible fluid may be regarded as due to a vortex sheet on the boundary (reference 10). In particular, for an axially symmetric body in a uniform flow parallel to its axis, the vortex sheet is simply a distribution of ring vortices along the surface having their axes coinciding with the body axis. Since for such a representation it can be shown that zero flow must exist at all points within the body itself (reference 11), it follows that the local surface velocity at any point on the body is equal to the local linear density of vorticity in the distribution of ring vortices.

Accordingly, once the surface velocity distribution has been determined for an axially symmetric body in a uniform flow parallel to its axis, the corresponding surface distribution of ring vortices is given immediately, and the determination of the perturbation flow velocity at any point in the neighborhood of the body reduces to an integration of the velocities due to ring vortices.

For a ring vortex the axial and radial induced velocity components u and v , respectively, are given by

$$u = \frac{\gamma}{2\pi r'} u^*$$

$$v = \frac{\gamma}{2\pi r'} v^*$$

where γ is the strength of the ring vortex and u^* and v^* are the induced velocity components for a ring vortex of any radius r' and corresponding strength $2\pi r'$ (or of unit radius and strength 2π). Charts of u^* and v^* as functions of x/r' and r/r' (replotted from reference 9) are shown in figures 1 and 2. Quantitative values of u^* and v^* may be obtained from figures 3 and 4 which were constructed from tables in reference 9. As may be seen by examination of figure 1, for a ring vortex rotating as indicated, the signs of u^* indicated in figure 3 are the same for positive values of x/r' as for negative ones. From figure 2 it may be seen that, for a ring vortex rotating as indicated, the signs of v^* in figure 4 are correct as shown for points in the first and fourth quadrants with respect to the ring vortex, considering the origin to be on the vortex axis, and are of opposite sign in the second and third quadrants. For a ring vortex whose sense of rotation is opposite to that indicated, of course, the signs are reversed for both u^* and v^* .

CALCULATION PROCEDURE

Incompressible flow.- The local flow-speed ratio V_1/V_0 and the flow angle ϕ at any point Q in the field of a cowl-spinner combination at zero incidence are given by

$$\frac{V_L}{V_0} = \sqrt{\left(1 + \frac{u}{V_0}\right)^2 + \left(\frac{v}{V_0}\right)^2}$$

$$\phi = \tan^{-1} \left(\frac{\frac{v}{V_0}}{1 + \frac{u}{V_0}} \right)$$

where

$$\frac{u}{V_0} = \int_{s_1}^{s_2} \frac{\frac{V_S}{V_0} u^*}{2\pi r'} ds + \int_{s_1'}^{s_2'} \frac{\frac{V_S}{V_0} u^*}{2\pi r'} ds'$$

$$\frac{v}{V_0} = \int_{s_1}^{s_2} \frac{\frac{V_S}{V_0} v^*}{2\pi r'} ds + \int_{s_1'}^{s_2'} \frac{\frac{V_S}{V_0} v^*}{2\pi r'} ds'$$

The quantities ds and ds' are increments of arc lengths along the cowling and spinner meridians, respectively. The limit s_1 refers to the point on the inner surface of the cowling farthest downstream from Q , s_2 to the point on the outer surface of the cowling farthest downstream from Q , s_1' to the point at the tip of the spinner, and s_2' to the point on the surface of the spinner farthest downstream from Q . The integration may be performed graphically, by plotting

$\frac{V_S}{V_0} u^*$ and $\frac{V_S}{V_0} v^*$ against s and s' and measuring the areas under the curves, or it may be performed numerically. Numerical methods of integration generally are considerably more rapid if many points of the flow field are to be calculated. For either system of integration the surface velocity ratios V_S/V_0 must be evaluated at a number of points R on the cowling and spinner surfaces and u^* and v^* must be evaluated at Q for the same points R . Usually a total of about 30 points is adequate; however, the actual number and location of the points R depend upon the location of Q and upon the shape of the surface velocity distribution. An example of a cowling-spinner combination with typical locations for the points R is shown in figure 5.

For an NACA 1-series cowl-spinner combination the values of V_S/V_0 for points R on the cowl nose, on the outer surface of the cowl, and on the surface of the spinner may be calculated from reference 7, where the corresponding pressure distributions are given, by the relation

$$\frac{V_S}{V_0} = \sqrt{1 - P}$$

For points R on the inner surface of the cowl and on the rearward extension of the spinner within the cowl, the surface velocities may be estimated on the basis of one-dimensional flow from the known annulus area and the given inlet-velocity ratio.

Values of u^* and v^* at Q for the various points R may be read from figures 3 and 4. As the distance between Q and R increases, the values of u^* and v^* rapidly approach zero; therefore, high accuracy in the values of V_S/V_0 beyond about 1 cowl diameter from Q is quite unnecessary and, in any case, the effect of points R beyond about 3 cowl diameters from Q may be neglected.

If the point Q is very close to the surface, the values of u^* and v^* corresponding to the nearest ring vortices become very large, and rather careful work is required to maintain adequate accuracy of the final result. Normally, however, this problem does not arise; the flow at the surface itself is presumably already known, and linear interpolation between the surface and the nearest point for which accurate results can readily be calculated should be adequate.

Compressible flow.— For a cowl-spinner combination with an inlet-velocity ratio of approximately unity, the compressible flow at a point Q, in a region where the deviations of the pressures from the free-stream conditions are small, may be estimated by the Prandtl-Glauert rule (one development of which is given in reference 12) as follows:

- (1) The coordinates of the cowl and spinner are stretched in the stream direction by the factor $\sqrt{1 - M^2}$.
- (2) The incremental velocities u'/V_0 and v'/V_0 in the stream and radial directions, respectively, are obtained for incompressible flow for the stretched body by the method outlined in the preceding section.
- (3) The incremental velocities of the unstretched body in compressible flow are calculated from the corresponding incremental velocities obtained in step (2) by the equations

$$\frac{u}{V_0} = \frac{u'/V_0}{1 - M^2}$$

and

$$\frac{v}{V_0} = \frac{v'/V_0}{\sqrt{1 - M^2}}$$

(4) The flow-speed ratio and flow angle are given by the same equations as those used in the preceding section.

At the present time no method exists whereby the compressible flow about a three-dimensional body may be obtained from the incompressible flow in a region where the deviation of the pressures from the free-stream pressure is large, nor are there available any experimental data on compressible-flow fields for three-dimensional bodies.

COMPARISON OF THEORETICAL AND EXPERIMENTAL RESULTS

The flow fields of several NACA 1-series cowlings configurations in essentially incompressible flow ($M = 0.13$) were determined experimentally in reference 13 by the use of bisecting centerplates aligned with the flow. (The NACA 1-series ordinates and an explanation of the designation system are given in reference 14.) The flow-speed ratios V_z/V_0 in the vertical plane of symmetry were obtained from pressure orifices installed on one side of the plate, and the flow angles ϕ were obtained from tufts installed on the other side of the plate.

The method of the present paper was used to calculate values of V_z/V_0 and ϕ in typical propeller-shank locations of three of these NACA 1-series cowlings-spinner combinations and one NACA 1-series open-nose inlet, and these calculated results are compared in figure 6 with the results obtained experimentally in reference 13. The agreement of the calculated values of V_z/V_0 with the experimental values is within $0.02V_0$ at all points in the fields where the comparisons were made. The agreement of the theoretical and experimental flow angles is also good at distances greater than about 25 percent of the maximum cowlings diameter from the cowlings nose; but nearer the cowlings nose, where it was more difficult to get accurate measurements of the high flow angles with the tufts, the agreement is not as close. However, a positive

check of the method is not essential for this particular application because, as pointed out in reference 13, propeller design is relatively insensitive to moderate variations in radial flow angles.

The method of the present paper is theoretically exact only for axially symmetric bodies at zero angle of attack. To obtain an approximation to the flow characteristics for an axially symmetric body at an angle of attack, however, the flows in the fields of the same NACA 1-series cowling configuration mentioned above were calculated for 10° angle of attack using the velocity distribution on the top of a cowling to obtain the perturbation velocities for the top, and using the velocity distribution on the bottom of the cowling to obtain the perturbation velocities for the bottom. Actually, this procedure neglects the effects of the circumferential variations of surface pressures on the flow characteristics.

The comparisons of the flow characteristics calculated by this approximate method with the results obtained experimentally are shown in figure 7. The agreement of the calculated and experimental results at radii greater than the maximum cowling radius is satisfactory. At distances nearer the axis of symmetry, the calculated flow-speed ratios generally are somewhat less than the experimental values on top of the axis of symmetry and are somewhat higher than the experimental values below the axis of symmetry; the differences between the calculated flow angles and the measured flow angles vary erratically near the nose.

The diameters of the cowlings and spinners were not increased by the displacement thicknesses of the boundary layers in these calculations; perhaps this refinement would have yielded closer agreement. In the case of the cowling at an angle of attack, it is reasonable to believe that as the angle approaches zero the calculated results will compare more favorably with the experimental values.

Langley Aeronautical Laboratory
National Advisory Committee for Aeronautics
Langley Field, Va.

REFERENCES

1. Fuhrmann, George: Theoretische und experimentelle Untersuchungen an Ballonmodellen. Jahrb. Jahrb. der Motorluftschiff-Studiengesellschaft Julius Springer (Berlin), 1911-1912, Vol. 5, pp. 65 - 123.
2. Von Kármán, Theodor: Calculation of Pressure Distribution on Airship Hulls. NACA TM No. 574, 1930.
3. Kaplan, Carl: Potential Flow about Elongated Bodies of Revolution. NACA Rep. No. 516, 1935.
4. Weinstein, Alexander: On Axially Symmetric Flows. Quarterly Appl. Math., vol. V, no. 4, Jan. 1948, pp. 429-444.
5. Betz, A.: Progress of the Calculative Methods. Part A, AVA Monographs, A. Betz, ed., Repts. and Translations No. 231, British M.A.P. Völkenrode, Oct. 1, 1946.
6. Küchemann, D.: Aerodynamics of Power-Plants. Repts. and Translations No. 61, British M.A.P. Völkenrode, May 1, 1946.
7. Boswinkle, Robert W., Jr., and Keith, Arvid L., Jr.: Surface Pressure Distributions on a Systematic Group of NACA 1-Series Cowlings with and without Spinners. NACA RM No. L8124, 1948.
8. Baals, Donald D., Smith, Norman F., and Wright, John B.: The Development and Application of High-Critical-Speed Nose Inlets. NACA ACR No. L5F30a, 1945.
9. Küchemann, D.: Tables for the Stream Function and the Velocity Components of a Source-Ring and a Vortex-Ring. Repts. and Translations No. 308, British M.A.P. Völkenrode, Nov. 15, 1946.
10. Lamb, Horace: Hydrodynamics. Reprint of sixth ed. (first American ed.), Dover Publications (New York), 1945, pp. 58, 59, 212, and 214.
11. Von Mises, Richard: The Theory of Flight. McGraw-Hill Book Co., Inc., 1945, pp. 197 and 224.
12. Gothert, B.: Plane and Three-Dimensional Flow at High Subsonic Speeds. NACA TM No. 1105, 1946.
13. Boswinkle, Robert W., Jr.: Air-Flow Surveys in the Vicinity of Representative NACA 1-Series Cowlings. NACA RM No. L8A15a, 1948.
14. Nichols, Mark R., and Keith, Arvid L., Jr.: Investigation of a Systematic Group of NACA 1-Series Cowlings with and without Spinners. NACA RM No. L8A15, 1948.

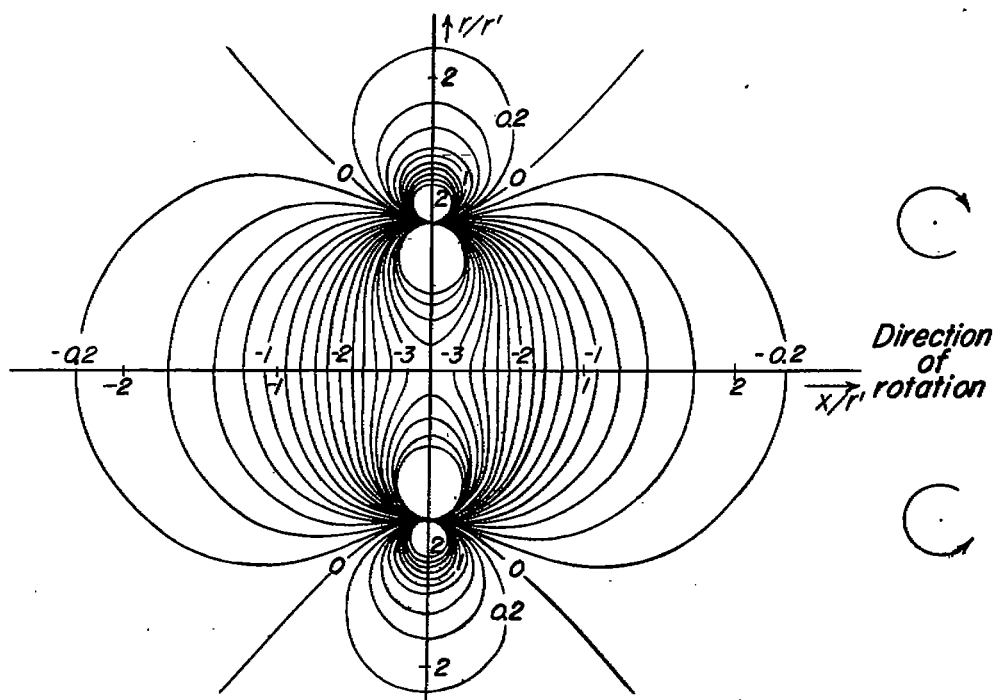


Figure 1.- Lines of constant axial velocity component u^* for a ring vortex of radius r' and strength $2\pi r'$.

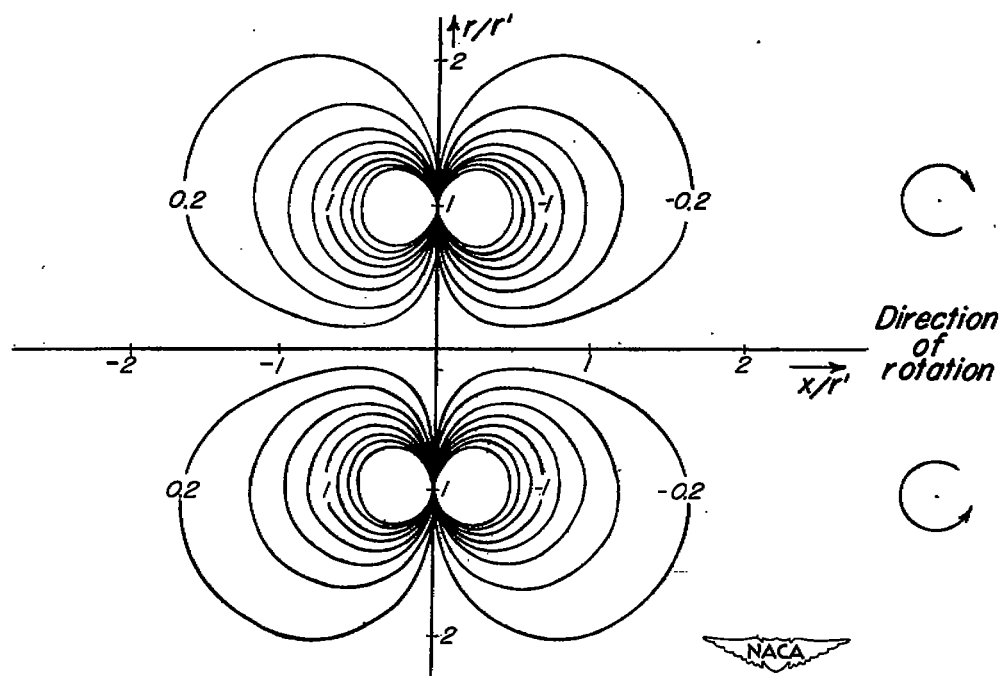
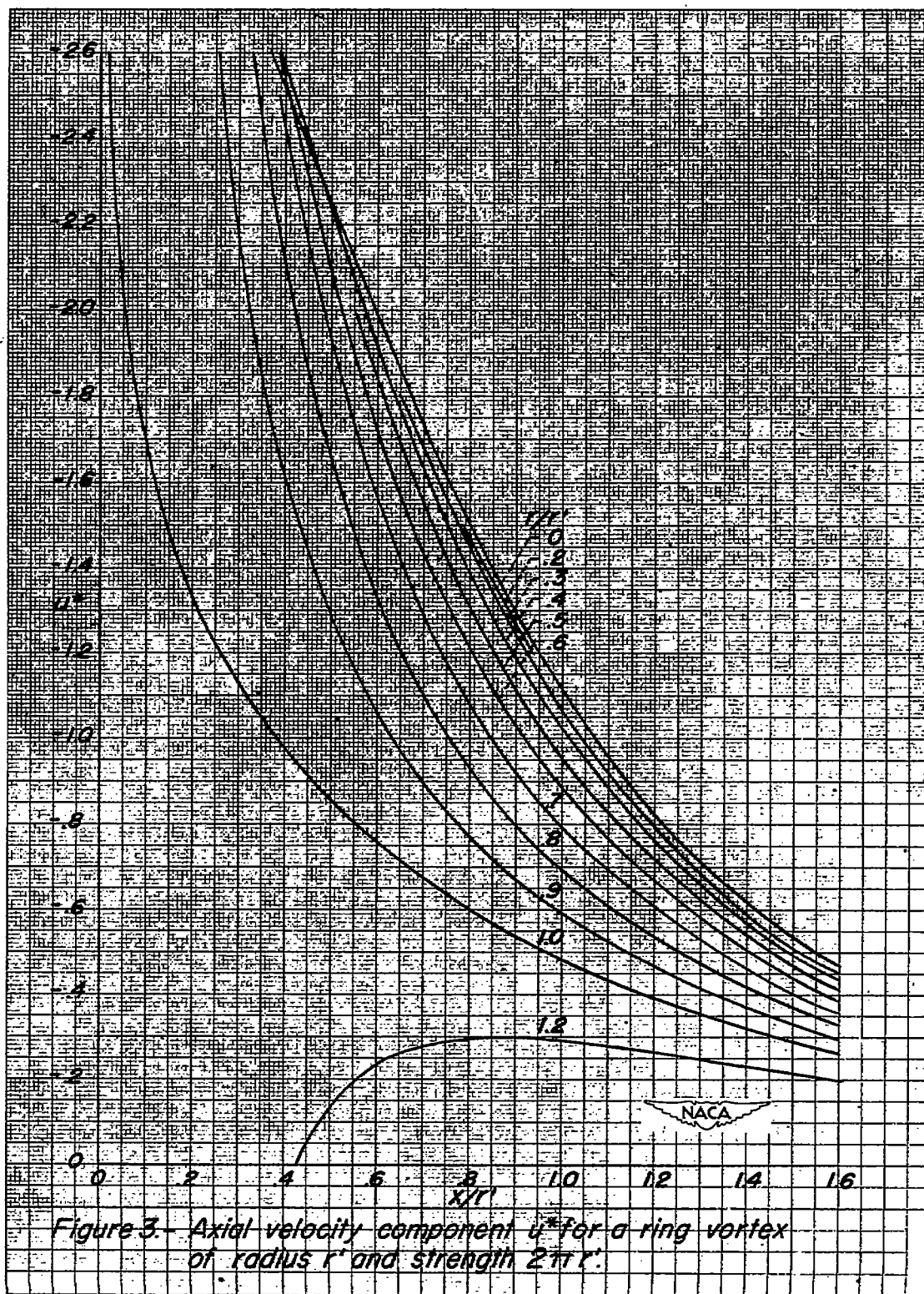
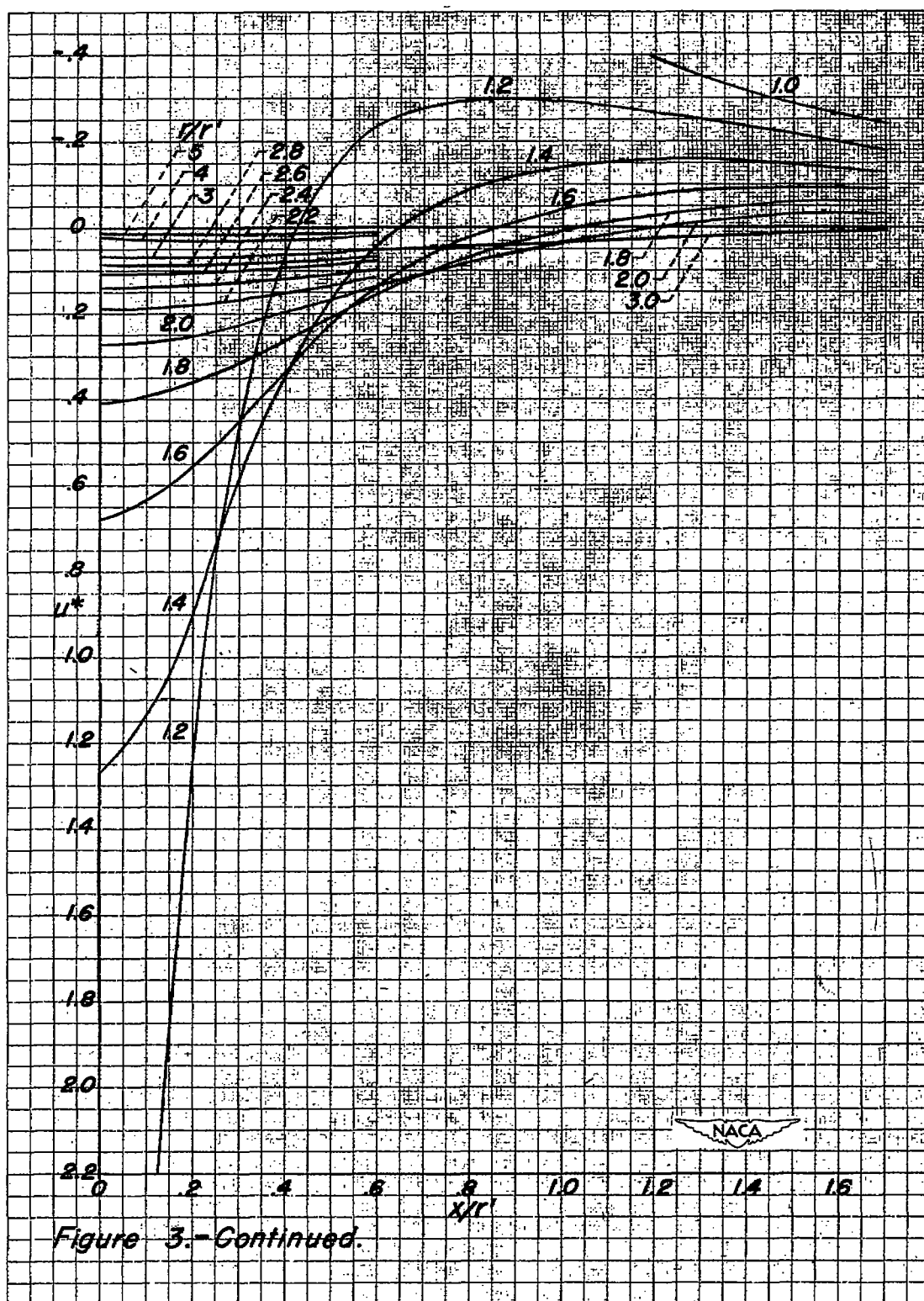


Figure 2.- Lines of constant radial velocity component v^* for a ring vortex of radius r' and strength $2\pi r'$.





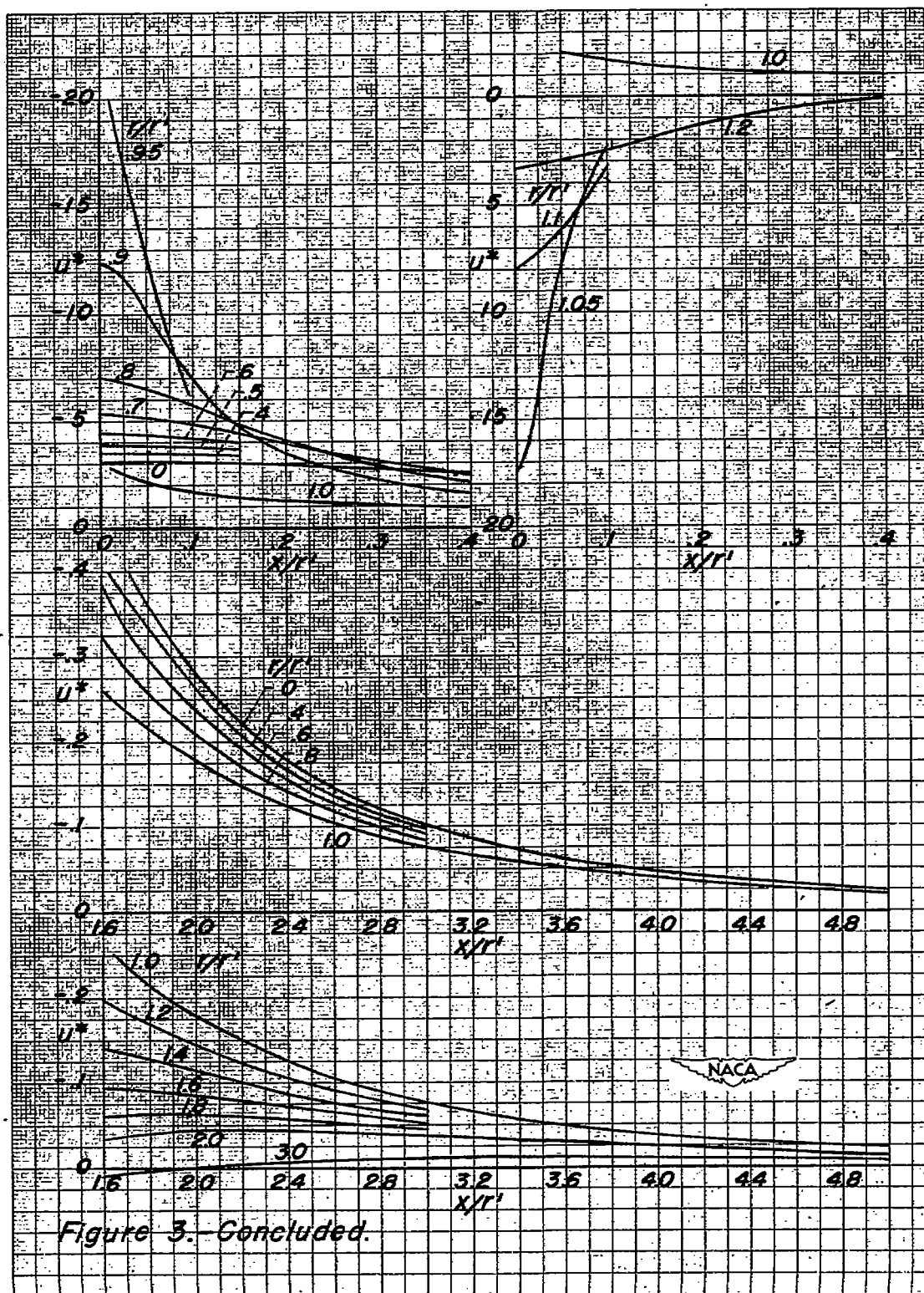
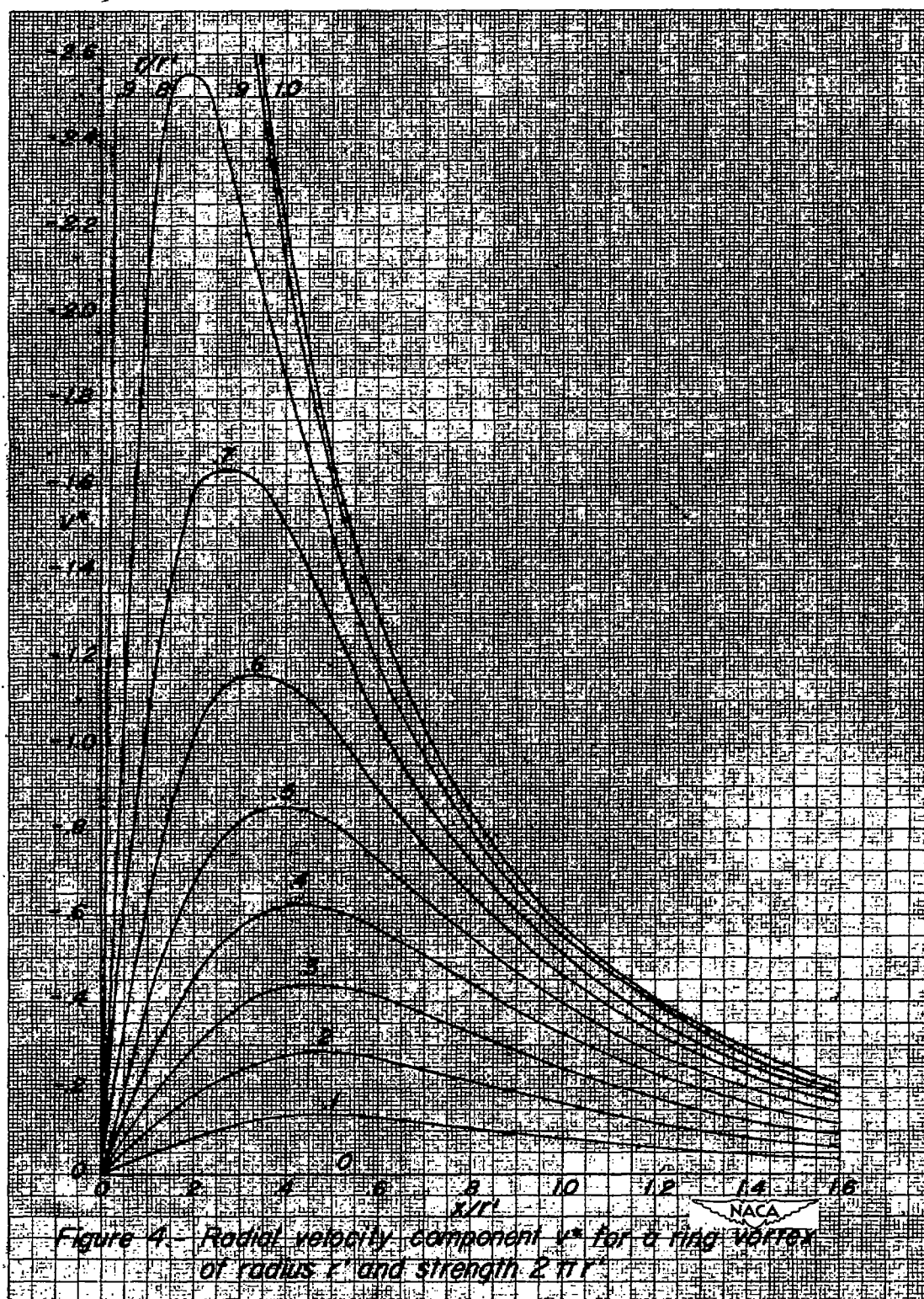
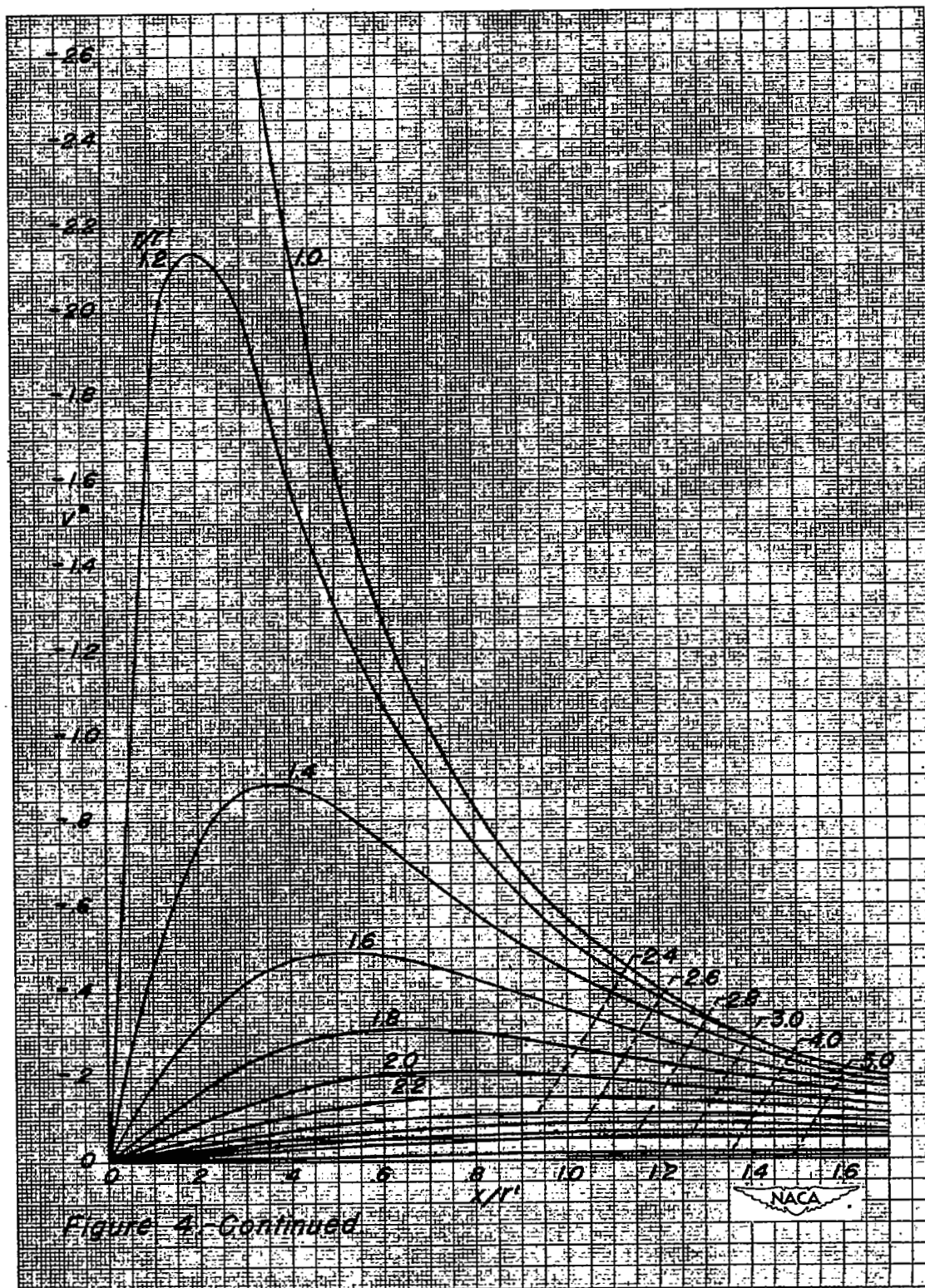


Figure 3. Concluded.





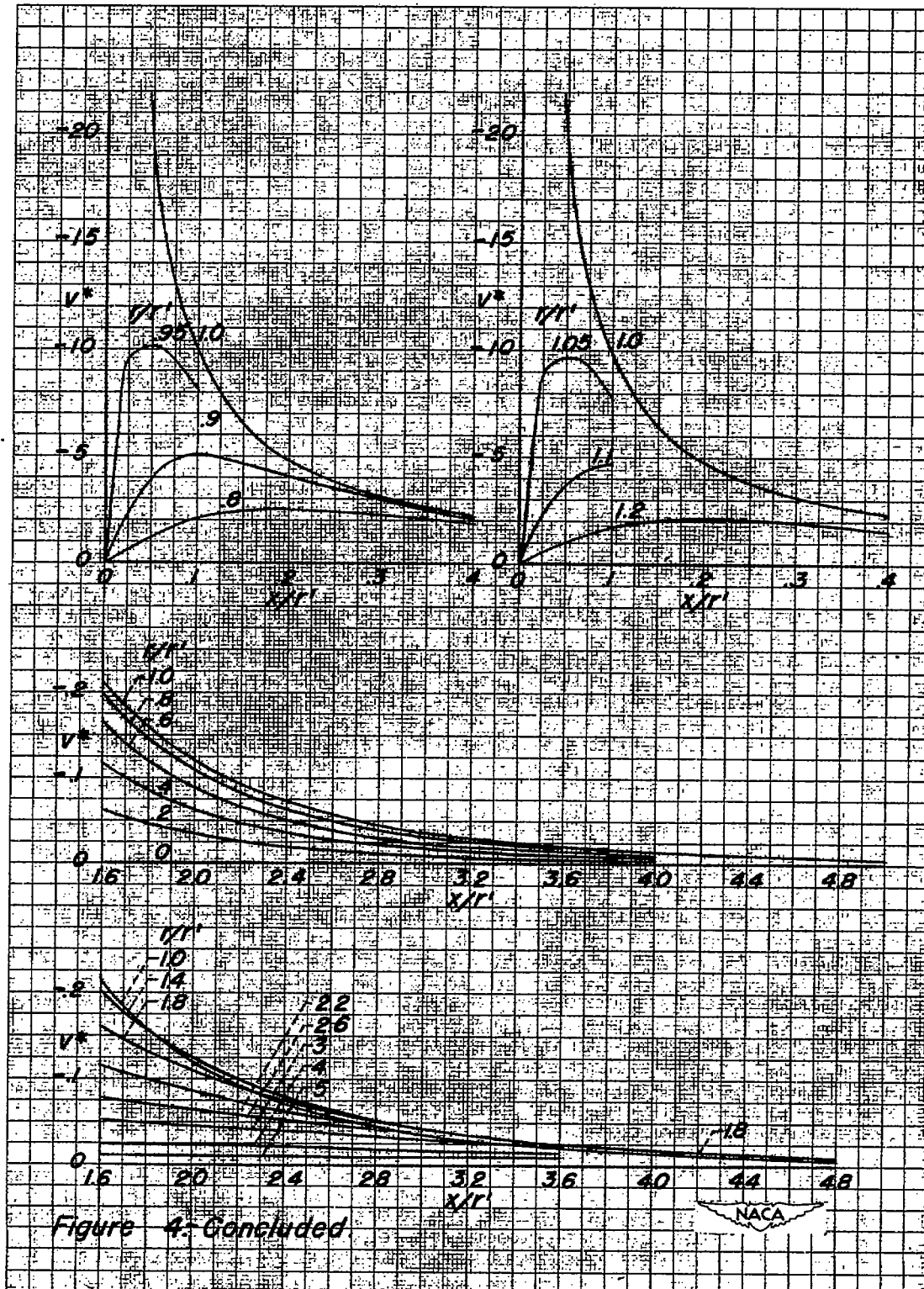


Figure 4. Concluded

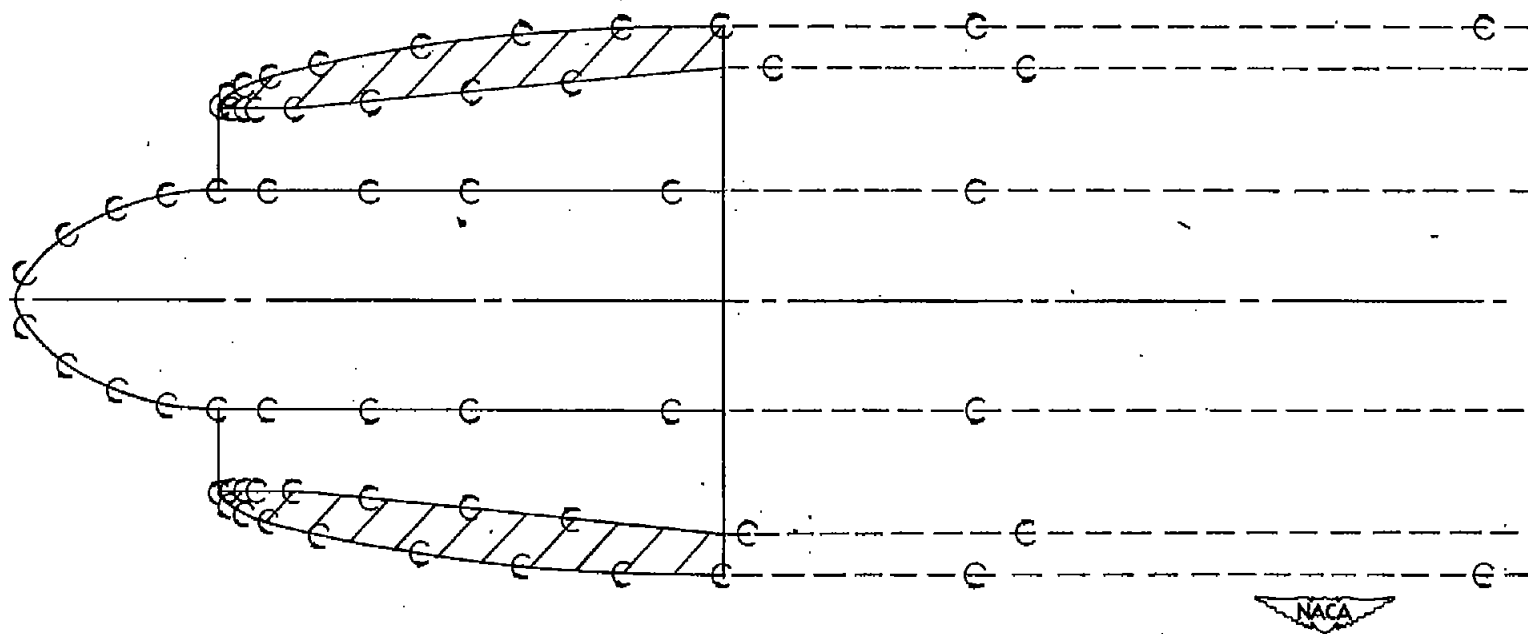
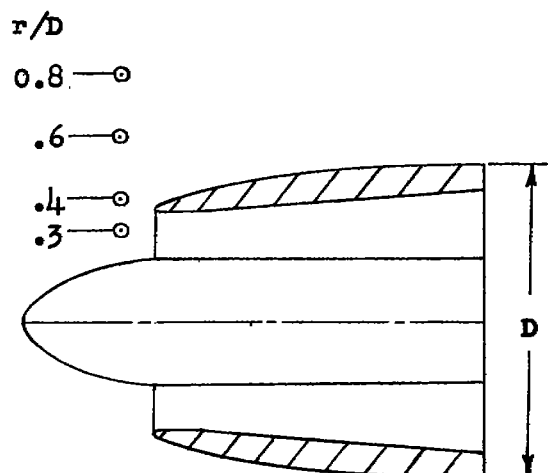
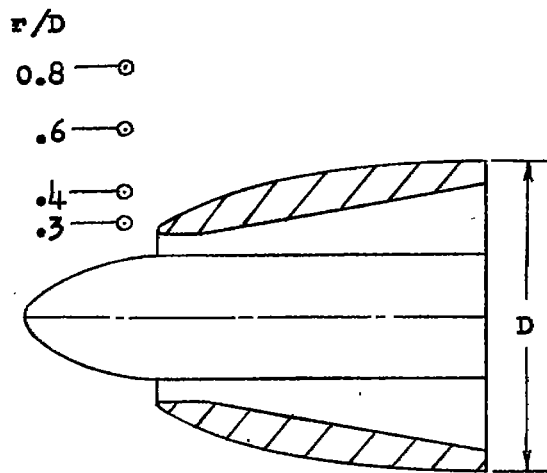


Figure 5.-Typical locations on cowling and spinner meridians for
chosen points R.



r/D	V_L/V_0		ϕ , deg	
	Calc.	Exp.	Calc.	Exp.
0.8	0.99	0.98	5	3
.6	.97	.96	8	5
.4	.88	.86	15	27
.3	.79	.80	14	23

(a) NACA 1-70-100 cowling with NACA 1-40-040 spinner; 0.1D upstream from inlet;
 $\frac{V_1}{V_0} = 0.63$.



r/D	V_L/V_0		ϕ , deg	
	Calc.	Exp.	Calc.	Exp.
0.8	0.99	0.99	5	0
.6	.97	.96	8	9
.4	.88	.88	15	25
.3	.81	.79	15	33


(b) NACA 1-55-100 cowling with NACA 1-40-040 spinner; 0.1D upstream from inlet;
 $\frac{V_1}{V_0} = 0.53$. 

Figure 6.- Comparison of flow characteristics calculated by theoretical method with values obtained experimentally; $\alpha = 0^\circ$. (Circles indicate points at which calculated and experimental results are compared.)

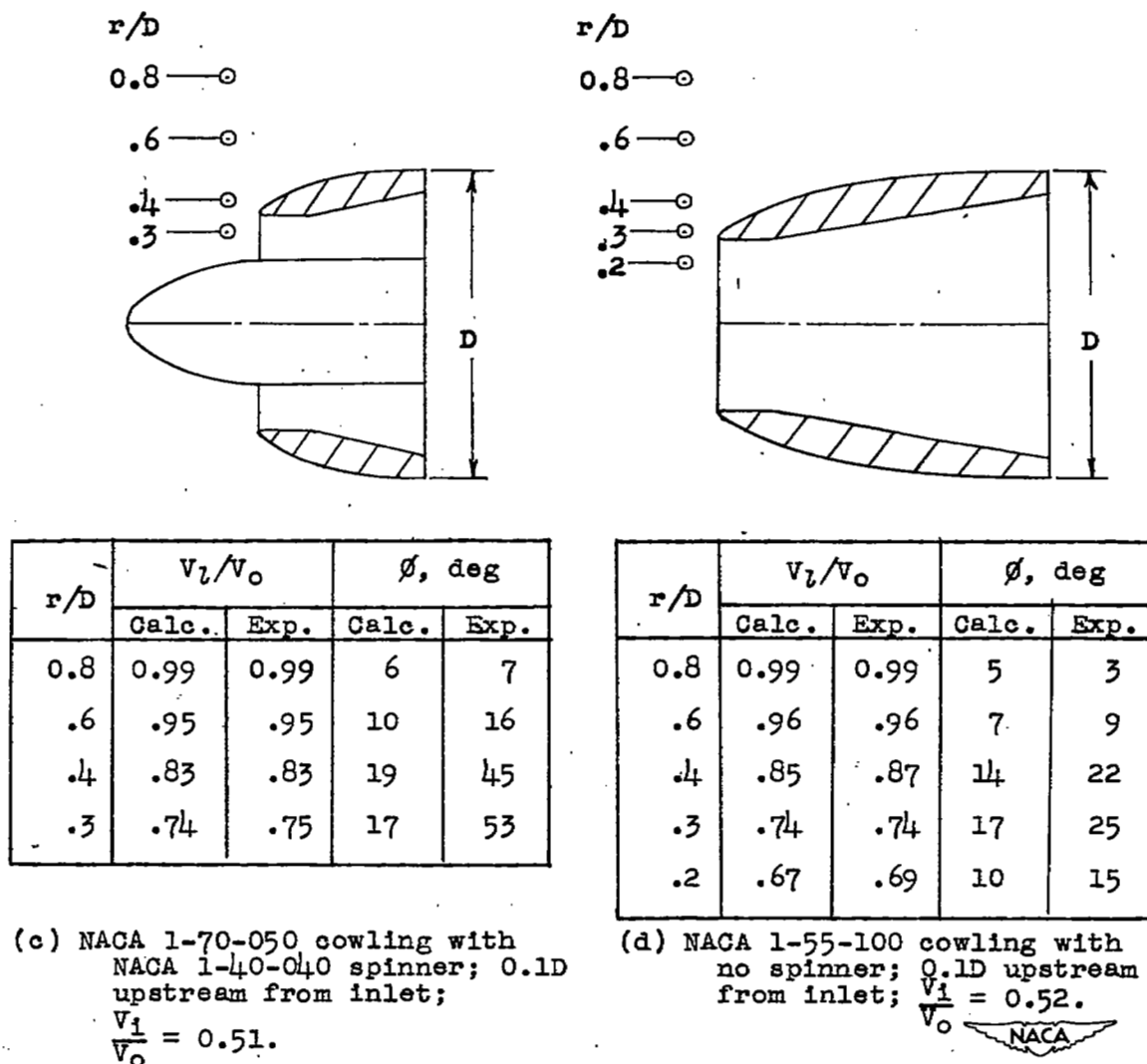
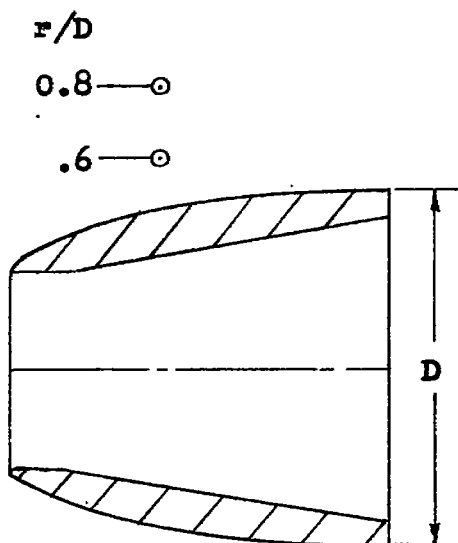


Figure 6.- Continued.

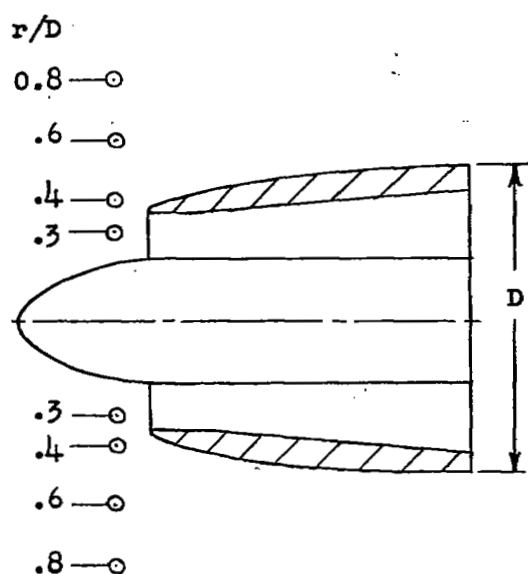


r/D	V_1/V_0		ϕ , deg	
	Calc.	Exp.	Calc.	Exp.
0.8	1.03	1.03	5	2
.6	1.06	1.06	8	9

(e) NACA 1-55-100 cowling with no spinner; $0.4D$ downstream from inlet; $\frac{V_1}{V_0} = 0.52$.

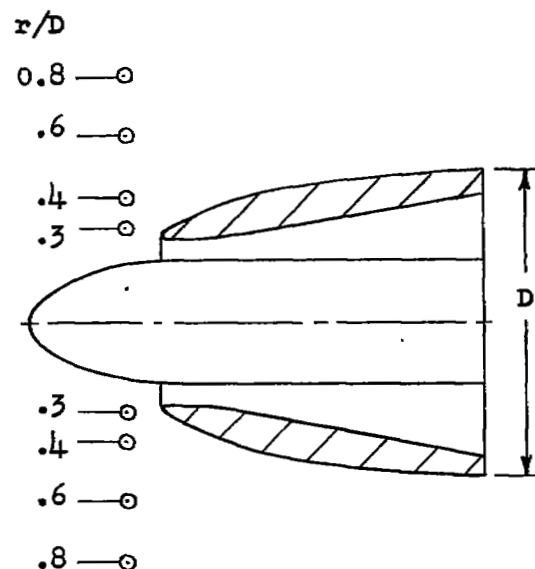


Figure 6.- Concluded.



r/D	V_1/V_0		ϕ , deg	
	Calc.	Exp.	Calc.	Exp.
<u>top</u>				
0.8	1.01	1.01	14	11
.6	.99	1.01	18	14
.4	.95	.95	23	20
.3	.88	.95	23	14
<u>bottom</u>				
.3	.98	.92	-8	-2
.4	.96	.86	-7	-3
.6	.94	.92	-6	-3
.8	.97	.95	-7	-3

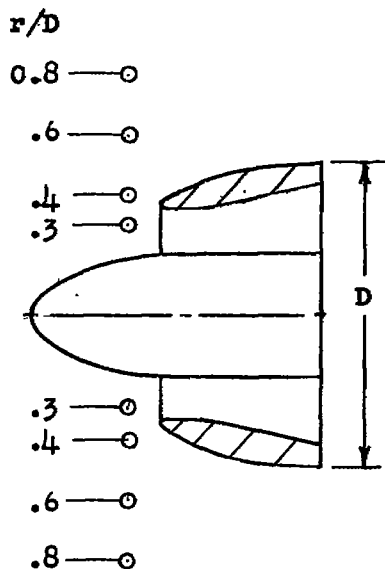
(a) NACA 1-70-100 cowling with NACA 1-40-040 spinner; 0.1D upstream from inlet;
 $\frac{V_1}{V_0} = 0.99$.



r/D	V_1/V_0		ϕ , deg	
	Calc.	Exp.	Calc.	Exp.
<u>top</u>				
0.8	1.02	1.02	15	10
.6	1.01	1.01	18	17
.4	.92	.98	24	23
.3	.84	.91	22	22
<u>bottom</u>				
.3	.96	.78	-5	6
.4	.86	.82	-3	10
.6	.94	.91	-4	2
.8	.97	.95	-7	0

(b) NACA 1-55-100 cowling with NACA 1-40-040 spinner; 0.1D upstream from inlet;
 $\frac{V_1}{V_0} = 0.93$.

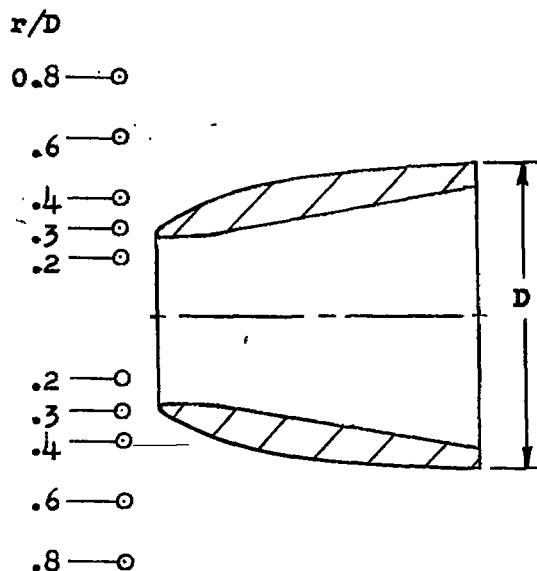
Figure 7.- Comparison of flow characteristics calculated by approximate method with values obtained experimentally; $\alpha = 10^\circ$. (Circles indicate points at which calculated and experimental results are compared.)



r/D	V_L/V_0		ϕ , deg	
	Calc.	Exp.	Calc.	Exp.
<u>top</u> 0.8	1.01	1.02	15	7
.6	1.01	1.02	19	10
.4	.90	.94	25	22
.3	.88	.95	22	6
<u>bottom</u> .3	.95	.84	8	0
.4	.87	.80	8	6
.6	.94	.88	5	2
.8	.97	.95	6	-4

(c) NACA 1-70-050 cowling with
NACA 1-40-040 spinner; 0.1D
upstream from inlet;

$$\frac{V_1}{V_0} = 1.00.$$

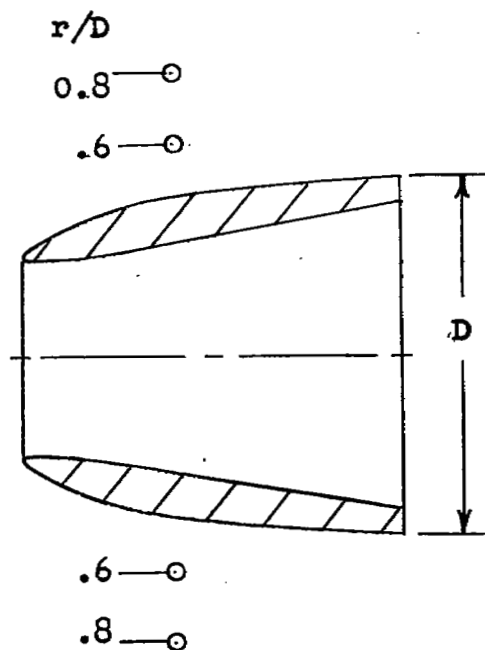


r/D	V_L/V_0		ϕ , deg	
	Calc.	Exp.	Calc.	Exp.
<u>top</u> 0.8	0.99	1.01	14	11
.6	.97	.99	17	16
.4	.87	.95	23	22
.3	.77	.88	17	19
.2	.79	.90	15	17
<u>bottom</u> .2	.92	.86	-12	-18
.3	.84	.77	-11	-14
.4	.83	.80	-5	2
.6	.92	.90	-6	2
.8	.96	.95	-7	-2

(d) NACA 1-55-100 cowling with
no spinner; 0.1D upstream
from inlet; $\frac{V_1}{V_0} = 1.02$.



Figure 7.- Continued.



r/D	V_L/V_0		ϕ , deg	
	Calc.	Exp.	Calc.	Exp.
<u>top</u> 0.8	1.02	1.05	5	8
.6	1.04	1.09	8	9
<u>bottom</u> .6	1.03	.99	8	7
.8	1.01	.98	5	1


(e) NACA 1-55-100 cowling with no spinner; 0.4D downstream from inlet; $\frac{V_1}{V_0} = 1.02$. 

Figure 7.- Concluded.

NASA Technical Library



3 1176 01436 6349